

³G. Ahlers and R. P. Behringer, *Prog. Theor. Phys.*, Suppl. **64**, 186 (1978).

⁴P. Atten and J. C. Lacroix, *J. Mec.* **18**, 469 (1979).

⁵J. C. Lacroix, P. Atten, and E. J. Hopfinger, *J. Fluid Mech.* **69**, 539 (1975).

⁶P. Atten, J. C. Lacroix, and B. Malraison, *Phys. Lett.* **79A**, 255 (1980).

⁷B. Malraison and P. Atten, in *Symmetries and Broken Symmetries*, edited by N. Boccara (IDSET, Paris, 1981), p. 439.

⁸B. Malraison and P. Atten, *C.R. Acad. Sci. Ser. B* **292**, 267 (1981).

⁹A. Bouabdallah, thesis, Nancy, 1980 (unpublished), and in Ref. 7, p. 407.

¹⁰M. Dubois, private communication.

¹¹J. P. Gollub, in *Proceedings of the Les Houches Summer School*, July 1981 (to be published).

¹²The concept of phase turbulence has been introduced theoretically by Y. Pomeau and P. Manneville, *Phys. Lett.* **75A**, 269 (1980), and observed in large- Γ experiments by P. Berge and M. Dubois, in *Systems Far from Equilibrium*, edited by L. Garrido, *Lecture Notes in Physics* Vol. 132 (Springer-Verlag, New York, 1980),

p. 381. Note that two other experiments can be connected with phase turbulence: that of J. E. Wesfreid and V. Croquette, *Phys. Rev. Lett.* **45**, 634 (1980), on phase diffusion and that of E. Guazelli, E. Guyon, and J. E. Wesfreid, in Ref. 7, p. 455, on defects in convective structure in a nematic hydrodynamic instability.

¹³G. Ahlers and R. P. Behringer, *Phys. Rev. Lett.* **40**, 712 (1978), and Ref. 3. See also Fig. 4 of A. Libchaber and J. Maurer, *J. Phys. (Paris)*, Lett. **39**, L369 (1978).

¹⁴P. Berge, in *Dynamical Critical Phenomena and Related Topics*, edited by C. P. Enz (Springer-Verlag, New York, 1979), p. 288. Figure 11 is compatible with an f^{-4} power-law spectrum.

¹⁵H. S. Greenside, G. Ahlers, P. C. Hohenberg, and R. W. Walden, to be published. See also B. Caroli, C. Caroli, and B. Roulet, *Physica (Utrecht)* **112A**, 517 (1982).

¹⁶U. Frisch and R. Morf, *Phys. Rev. A* **23**, 2673 (1981).

¹⁷P. Manneville, *Phys. Lett.* **84A**, 129 (1981).

¹⁸J. P. Gollub, S. V. Benson, and J. F. Steinmann, *Ann. N.Y. Acad. Sci.* **357**, 22 (1980).

¹⁹Y. Pomeau, private communication.

Nonlinear Pattern Formation near the Onset of Rayleigh-Bénard Convection

H. S. Greenside, W. M. Coughran, Jr., and N. L. Schryer

Bell Laboratories, Murray Hill, New Jersey 07974

(Received 23 June 1982)

It is shown that many of the experimentally observed features of pattern formation in Rayleigh-Bénard convection near onset can be understood in terms of a two-dimensional relaxational equation. In particular, it is shown that disordered roll patterns follow a complicated dynamics that can require up to a hundred horizontal diffusion times to reach equilibrium.

PACS numbers: 47.25.Mr

In attempting to understand the essential ways in which nonlinear nonequilibrium systems become turbulent, considerable experimental and theoretical effort has been devoted to one of the simplest systems, Rayleigh-Bénard convection.¹ While a fairly satisfactory understanding has emerged for small-aspect-ratio cells,² no such understanding currently exists for the onset of turbulence in large-aspect-ratio cells, whose large lateral dimensions (compared with the depth of the fluid) allow the excitation of long-wavelength modes and the presence of defects. An experiment in a large cylindrical cell shows chaotic behavior at the onset of convection³ while a recent experiment in a large rectangular cell⁴ suggests that the fluid becomes clearly time de-

pendent only a finite distance above onset. Theory predicts that parallel rolls within a certain band of wave numbers are stable but makes no prediction of the possible time dependence of curved or disordered rolls.

In this Letter, we use a two-dimensional equation⁵ to study numerically the evolution and formation of curved roll patterns (corresponding to three-dimensional flow in the fluid) in large rectangular cells just above the onset of convection. Our model accurately reproduces the physics of the Boussinesq equations¹ sufficiently close to onset and for sufficiently large-aspect-ratio cells. Unlike most experiments to date, we determine *both* the Nusselt number and the velocity field as functions of time, permitting a more quantitative

comparison of theory with the thermal measurements of Ref. 3 and the visual observations of Ref. 4. Although the model we use is relaxational and incapable of truly nonperiodic behavior, we find for disordered roll patterns complicated long-lived transients which could be misconstrued in optical measurements to be turbulence if observed over short time scales.

Our numerical solutions also provide explicit examples of how, in a simple model, lateral boundaries and nonlinear terms select among the various highly degenerate solutions to the linear problem.⁶ These results will be of interest for studying pattern formation in related problems in which a continuous instability occurs at a finite wave number.

Near onset the Boussinesq equations can be systematically expanded in the small parameter $\epsilon = (R - R_c)/R_c$, where R is the Rayleigh number and R_c is the critical Rayleigh number for a laterally infinite container. As first shown in Ref. 5, the amplitude equation resulting from the lowest-order solvability condition for this expansion⁷ can be made rotationally invariant by using a real amplitude, $\psi(x, y, \tau)$, which includes the rapid spatial oscillations of the rolls. Here x and y are the physical spatial variables and $\tau = \epsilon t$ is a slow time variable. The equation and boundary conditions for ψ are⁸

$$\partial_\tau \psi = \epsilon \psi - (\Delta + q_0^2) \psi - \psi^3, \quad (1)$$

$$\psi = \partial_n \psi = 0, \quad (2)$$

where $\Delta = \partial_{xx} + \partial_{yy}$ is the Laplacian, q_0 is the critical wave number minimizing R_c , and ∂_n is the derivative normal to the boundary. (In what follows, we set $q_0 = 1$ so that a roll diameter is 2π). This equation is valid for the experimentally attained case of rigid (nonslip) surfaces⁹ but was recently shown to be incorrect for small Prandtl numbers and for free surfaces for which the generation of vertical vorticity must be taken into account.¹⁰ An important property of Eq. (1) is that it is variationally derived from a Lyapunov functional,

$$F[\psi] = \frac{1}{2} \int dx dy \left\{ -\epsilon \psi^2 + \frac{1}{2} \psi^4 + [(\Delta + 1)\psi]^2 \right\}, \quad (3)$$

which decreases monotonically for all initial conditions.⁸ Equation (1) is then purely relaxational and any solution tends towards a time-independent state which can be metastable or stable depending on whether the corresponding value of Eq. (2) is a local or global minimum.

We have numerically solved Eq. (1) with the

boundary conditions, Eq. (2), for rectangular geometries with both random positive and negative domains or parallel rolls for initial conditions and for different values of ϵ . Details concerning our numerical method will be presented elsewhere.¹¹

For large aspect ratios ($\Gamma = L \gg 1$, where L is the smaller lateral dimension) and for small ϵ [$\epsilon_c \ll \epsilon \ll 1$, where $\epsilon_c \cong (2\pi/\Gamma)^2$ is the smallest ϵ for which nonzero solutions are stable], the initial amplitude evolves to a pattern such that most rolls are normal to the boundaries (see Fig. 1). This is in agreement with experiment⁴ and with the analysis of Ref. 8. For initial conditions consisting of parallel rolls at the critical wave number $q_0 = 1$, a cross-roll instability eliminates rolls parallel to the lateral boundary by creating local rolls, also of wave number 1, perpendicular to those sides [see Fig. 1(a)]. This was first predicted by Pomeau and Zaleski¹² and has not yet been clearly observed in experiments. This instability is confined to a boundary layer⁸ of thickness $2\pi\epsilon^{-1/2}$; we find that the cross rolls are stable to perturbations and do not grow into the interior although the state, Fig. 1(a), is metastable [Fig. 1(b) has a lower Lyapunov value, Eq. (2)]. As seen in Figs. 1(b), 1(d), and 1(e), normality to the boundaries is frequently achieved by forming roughly concentric rolls with a corner as the focus. A new feature not previously observed or predicted is the tendency of the rolls to form a domain of straight segments away from the lateral boundaries [see Figs. 1(b) and 1(e)]. We predict that truly circular concentric rolls, such as those discussed in Ref. 8, do not occur at low Rayleigh number.

For random initial conditions, the smallest length scales anneal out rapidly on the order of a vertical diffusion time [$\tau \sim 1$ in the units of Eq. (1)] and rolls normal to all boundaries grow in towards the center of the cell, creating a disordered texture. There then follows a long and complicated evolution in which the pattern simplifies through migration and annihilation of defects in a manner similar to that described in the experiments of Ref. 4 [see Fig. 1(e), an intermediate state, which evolves into the stationary state, Fig. 1(f)]. The primary mechanism of defect motion is gliding perpendicular to the roll axis. The final equilibrium state favors defects or grain boundaries at corners or along the shorter sides [Figs. 1(b) and 1(f)], although during evolution quite complicated defects such as disclinations occur [see the lower right corner of

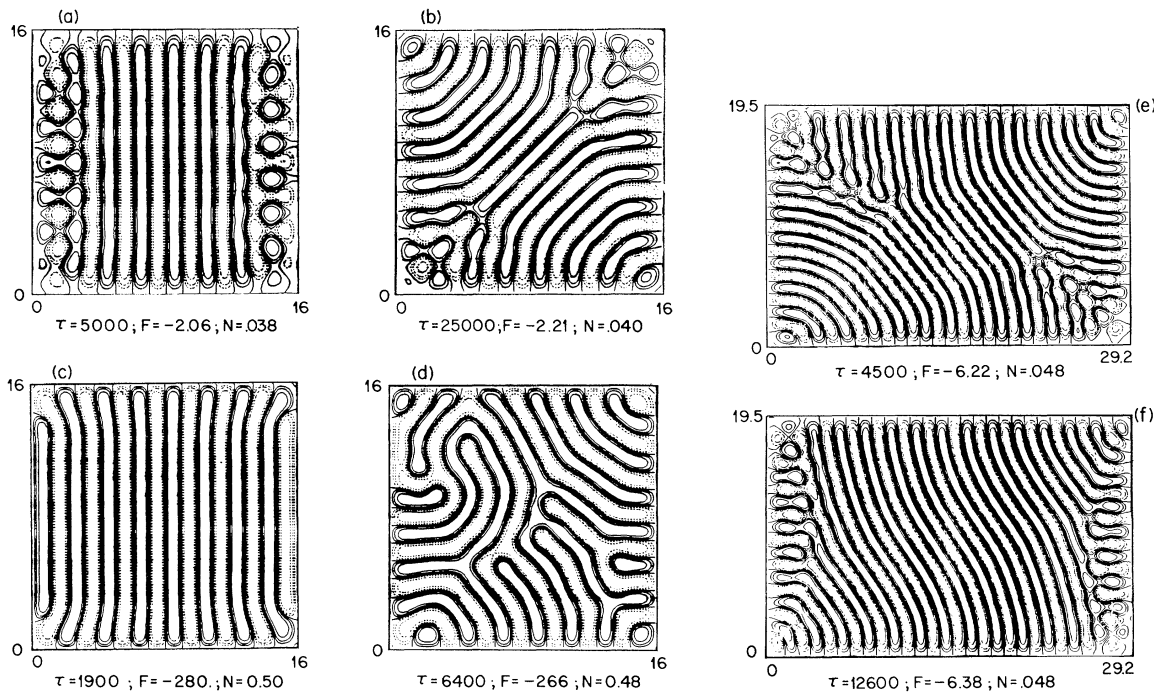


FIG. 1. Contour plots of the amplitude field, $\psi(x, y, \tau)$, at various times for (a), (b), (e), and (f) $\epsilon = 0.10$ and (c) and (d) $\epsilon = 0.90$. The cells in (a)–(d) have an aspect ratio of 16 while the cells in (e) and (f) have aspect ratios of 29.2 and 19.5 to match the cell of Ref. 4. The initial conditions were parallel rolls for (a) and (c) and random domains of opposite sign for (b) and (e). The solid and dotted contours represent positive and negative values at $\frac{1}{2}$, $\frac{1}{4}$, $\frac{1}{8}$, and $\frac{1}{16}$ the maximum amplitude. The contours correspond to vertical velocity contours in optical experiments. The values of the time at which equilibrium was reached (τ), the Lyapunov functional (F), and the Nusselt number (N) are given. The state in (e) has not reached equilibrium and is evolving into the equilibrium state, (f). Here equilibrium is defined to occur when $d \ln(F)/d\tau$ is smaller than 10^{-8} .

Fig. 1(e)]. The normality of the rolls to the boundaries and the low density of defects in the stationary state are consistent with the theoretical analysis of Ref. 8. A repeated run on both the square and rectangular cells of Fig. 1 with $\epsilon = 0.1$ but with different random initial conditions also leads to the states shown in Figs. 1(b) and 1(f) which suggests that, for small ϵ , the nonlinear term and confining lateral walls select one from the large multiplicity of states suggested by a linear analysis.⁶

Although the derivation of Eq. (1) is physically meaningful only for small ϵ , we have also investigated its solutions for larger ϵ in which case qualitatively different pattern formation occurs. For $\epsilon = 0.9$ and $\Gamma = 16$, parallel rolls relax only a little and the cross-roll instability is suppressed [see Fig. 1(c)]. This seems related to the fact that the boundary layer is now less than a roll diameter. The symmetry of the state, Fig. 1(c), and its low Lyapunov value [compare Fig. 1(d)] suggest that this is the most stable state for this

value of ϵ . Indeed if the state of Fig. 1(b) is used as an initial condition for a run with $\epsilon = 0.9$, the pattern remains essentially unchanged and the Lyapunov functional decreases to a value of $F = -275$, still greater than that of Fig. 1(c). Random initial conditions lead to disordered textures such as the equilibrium state, Fig. 1(d), which are more highly curved and have a higher density of defects than the low- ϵ equilibrium states. The evolution to the state in Fig. 1(d) is highly constrained or “frozen” in that after the annealing out of small length scales, the texture essentially has reached equilibrium. This corresponds to falling into the nearest of many local minima of the Lyapunov functional, Eq. (2). If the stationary state of Fig. 1(d) is used as an initial condition for a run with $\epsilon = 0.1$, the texture rapidly “melts” and evolves towards the state in Fig. 1(b). This suggests that disordered textures are most readily annealed by bringing the Rayleigh number close to the critical value, R_c .

The time evolution for the large cells of Figs.

1(b) and 1(f) confirms the experimental observation⁴ that the time scale for reaching equilibrium starting from a disordered pattern is often an order of magnitude or more greater than a horizontal diffusion time ($\tau \gg \Gamma^2$). These results also demonstrate that complicated defect motion can occur without taking into account the generation of vertical vorticity.¹³ A careful examination of the value of the Lyapunov functional as a function of time during these runs showed that it is *strictly decreasing* at all times. This rules out the possibility that the long time scale arises from rare computer-noise-induced transitions (over barriers significantly larger than the integrating accuracy), from metastable to successively lower states. Instead, this behavior must arise from a complicated dynamics in a large phase space (the "glass" hypothesis of Ref. 10). Presumably the same conclusion holds for experiment. The numerical evidence is insufficient to determine whether the time scale for attaining equilibrium scales with Γ^2 . We have also studied as a function of time the Nusselt number, $N = 1 + (1 + \epsilon)^{-1} \times \langle \psi^2 \rangle$ where $\langle \dots \rangle$ denotes an average over horizontal coordinates. The Nusselt number turned out to be a strictly *increasing* function of time so that, in this model, the equilibrium state is the one which maximizes the heat transport from the lower to upper plate. These results are incompatible with the clearly nonrelaxational time dependence observed immediately above onset in large cylindrical cells.³ More experiments and numerical studies¹⁴ will be needed to determine whether a combination of cylindrical geometry and higher-order terms can produce this turbulence.

In summary, our numerical investigation of a relaxational amplitude equation confirms many of the observed features of pattern formation near onset in large rectangular cells, especially that a long time may be needed to reach a stationary state. It would be fruitful to investigate experimentally some of the predictions suggested by our model (especially in high-Prandtl-number

fluids and for Rayleigh numbers below the onset of secondary time-dependent instabilities¹) such as the confinement of the cross-roll instability to a boundary layer of size $\epsilon^{-1/2}$, the monotonically increasing Nusselt number, the specific lowest Lyapunov states of Figs. 1(b) and 1(f), the formation of straight roll domains away from the boundary layer, and the increasing rigidity and density of defects for higher- ϵ patterns.

We wish to thank M. C. Cross for suggesting the investigation of Eq. (1) and him, P. Hohenberg, and J. Gollub for many stimulating and critical comments. We also thank D. J. Rose for useful suggestions concerning the numerical code, and P. Bjørstad for the use of his fast biharmonic solver which was central to our effort.

¹J. P. Gollub, in *Nonlinear Dynamics and Turbulence*, edited by D. Joseph and G. Iooss (Pittman, New York, 1982); F. H. Busse, *Rep. Prog. Phys.* **41**, 1929 (1978).

²J. P. Eckmann, *Rev. Mod. Phys.* **53**, 643 (1981).

³G. Ahlers and R. P. Behringer, *Prog. Theor. Phys.*, Suppl. **64**, 186 (1979); G. Ahlers and R. Walden, *Phys. Rev. Lett.* **44**, 445 (1980).

⁴J. P. Gollub and J. F. Steinman, *Phys. Rev. Lett.* **47**, 505 (1981); J. P. Gollub, A. R. McCarrier, and J. F. Steinman, to be published.

⁵J. Swift and P. C. Hohenberg, *Phys. Rev. A* **15**, 319 (1977).

⁶C. Normand, *J. Appl. Math. Phys.* **32**, 81 (1981).

⁷A. C. Newell and J. A. Whitehead, *J. Fluid Mech.* **38**, 279 (1969); L. A. Segel, *J. Fluid Mech.* **38**, 203 (1969).

⁸M. C. Cross, *Phys. Rev. A* **25**, 1065 (1982).

⁹M. C. Cross, *Phys. Fluids* **23**, 1727 (1980).

¹⁰E. D. Siggia and A. Zippelius, *Phys. Rev. Lett.* **47**, 835 (1981).

¹¹P. Bjørstad, W. M. Coughran, Jr., H. S. Greenside, D. J. Rose, and N. L. Schryer, to be published.

¹²Y. Pomeau and S. Zaleski, *J. Phys. (Paris)* **42**, 515 (1981).

¹³E. D. Siggia and A. Zippelius, *Phys. Rev. A* **24**, 1036 (1981).

¹⁴Some numerical solutions of Eq. (1) in cylindrical cells have been obtained by P. Manneville, to be published.